Rheol Acta 34:544–561 (1995)

ORIGINAL CONTRIBUTION

James Z. Q. Zhou
Tunan Fang
Guihua Luo
Peter H. T. Uhlherr

Yield stress and maximum packing fraction of concentrated suspensions

Received: 10 January 1995
Accepted: 23 August 1995

J. Z. Q. Zhou · Prof. P. H. T. Uhlherr (✉)
Department of Chemical Engineering
Monash University
Clayton 3168, Australia

Fang Tunan Luo
Department of Chemical Engineering
East China University
of Science & Technology
Shanghai 200237, P. R. China

Abstract The yield stress and features of the structure of concentrated suspensions based on silica flour, with particles of average diameter around 4 μm, were investigated in terms of a phenomenological model. The yield stress of a concentrated suspension of known solid volume concentration is estimated by employing a shear-dependent maximum packing fraction ϕ_m which is obtained by model fitting equilibrium viscosity data, and by incorporating a first-order kinetic equation. The model proposed was examined by using several mineral suspensions in which silica flour was mixed with metal oxide particles so that microstructural features of the suspensions could be adjusted. A cocoa fat suspension was also used as a test sample having radically different chemistry. The agreement between the model prediction and independently obtained experimental evidence is acceptable. Furthermore, a qualitative explanation is obtained by a scaling analysis in an effort to relate the model parameters with the suspension structure that stems from interactions among the suspension constituents.

Key words Concentrated suspension – maximum packing fraction – yield stress – suspension structure

Introduction

Solid-liquid suspensions containing a high volume concentration of solid particles are frequently encountered in manufacturing processes and in transport. In order to deal with these suspensions rationally and effectively, it is important to achieve desirable rheological properties, and these depend critically upon an understanding of suspension behaviour during processing. In order to understand the diverse behaviours of suspensions in an actual process, we need detailed information on the nature of the suspension constituents, i.e., the characteristics of suspended solid particles and suspending liquid medium. We also need to know details of interactions among these suspension constituents. This is because the diverse behaviour observed for concentrated suspensions including their rheology, derives almost entirely from structural variety introduced by interactions between the particles or aggregates themselves and between the particles and the liquid medium. In addition, the environment where the particle interactions actually occur, and which is determined by the properties of the suspending medium, should be well-defined so that the forces involved in particulate interactions can be identified in terms of existing rheological theories and experimental techniques.

Our knowledge of suspension rheology is still too incomplete to achieve an adequate understanding and a detailed description of the complex behaviour of highly concentrated suspensions. However, enormous progress both in theoretical description and experimental measurements has been made in recent years for well-characterised systems containing uniform spherical particles at higher concentration (Mooney, 1951; Krieger and Dougherty, 1959; Frankel and Acrivos, 1967; Russel, 1980; Frith et al., 1987; Buscall, 1991). Significant pro-

RA 721

gress has also been made for concentrated bimodal suspensions (Farris, 1968; Chong et al., 1971; Sengun and Probstein, 1989; Chang and Powell, 1993; Probstein et al., 1994). For concentrated suspensions containing polydispersed particles, some work has been done experimentally to investigate the effect of suspended particle properties on the rheology (Dabak and Yucel, 1986; van der Werff and de Kruif, 1989; Tsai et al., 1992) and the effect of suspending medium properties on the rheology and stability (Tsai and Viers, 1987; Tsai et al., 1989; Leong and Boger, 1990; Chang et al., 1993). Some work has been reported on modeling concentrated suspensions containing polydispersed particles as well as having a yield stress (Quemada, 1984; Wildemuth and Williams, 1984; Doraiswamy et al., 1991).

The purpose of this paper is to present a phenomenological approach by which the yield stress of a concentrated suspension of known solid volume concentration can be estimated using a shear-dependent maximum packing fraction ϕ_m. The essential features of the approach are highlighted. The method of acquiring model parameters is described, and a scaling analysis is presented to correlate these parameters with the properties of the suspension constituents and thus to identify the relative importance of forces that exist in suspensions. The factors that affect the value of maximum packing fraction, and through this, the predicted yield stress, are given and discussed. Yield stress values obtained using this approach are compared with independent measurements such as vane torsion and extrapolation of flow curve.

Maximum packing fraction (ϕ_m)

Maximum packing fraction is the volume fraction of aggregates in closest-packing at which the relative viscosity approaches infinity. Interpretation of maximum packing fraction has varied with time and with the circumstances in which it is being applied. It is, initially, defined only as a geometrical constant in a mono-dispersed particle system, and is later considered as a closer-packed volume fraction being responsive to particle properties such as particle shape and distribution of particle size (Chong et al., 1971; Dabak and Yucel, 1986). Maximum packing fraction, at present, is regarded as a variable corresponding to a given collection of particles under given conditions of flow (Wildemuth and Williams, 1984), and is believed to be a representation of the actual structure of a suspension (Quemada, 1984).

Evaluation method

Analytical calculation

Maximum packing fraction, as a geometric parameter, may be calculated provided the type of particle packing is clear. Certainly, its value varies with shape of particle and distribution of particle size and depends critically upon the assumed type of particle packing. An analytical method first proposed by Lee (1970) and then improved by Patton (1979) can be used for calculating maximum packing fraction in relation to the packing of spheres with various size distributions based on the idealized packing characteristics of binary mixtures. Unfortunately, the actual type of particle packing is unknown in most cases so that the analytical method for calculating maximum packing fraction results in poor agreement between different data sets. Therefore, many investigators suggested that there exists a range of maximum packing fractions (Maron and Krieger, 1960; Nielsen, 1977; Ackerson, 1990; Shapiro and Probstein, 1992). Clearly, it is rather unrealistic to imagine that maximum packing fraction of a concentrated suspension can be evaluated from particle properties and an assumed type of particle packing in the absence of a flow model.

Graphical extrapolation of experimental data

Maximum packing fraction of a concentrated suspension may be obtained by extrapolation of experimental data from rheometers. It is worth noting that the reliability of the maximum packing fraction obtained by this method is dependent on the ability to measure extremely large relative viscosities of highly concentrated suspensions for which many problems could arise due mainly to the inhomogeneous sample, unexpected rupture of sample structure at relatively high shear, and slip phenomena, even using a measuring system having grooves. As a consequence, this method is considered to contain great uncertainties because of limited data in the vicinity of maximum packing fraction, although it has certain advantages such as the fact that it is straightforward, simple in principle.

Sedimentation by gravity and centrifuge

The principal method used for measuring maximum packing fractions of concentrated suspensions is sedimentation by gravity or centrifuge. Many investigators estimated the value of the maximum packing fraction by sedimentation experiments (Kao and Nielson, 1975; Poslinski et al., 1988; Chiu and Don, 1989). It is noted that this method does not take the effects due to various states of particle aggregation into account. The single

Rheologica Acta, Vol. 34, No. 6 (1995)

value of maximum packing fraction obtained by gravity sedimentation or centrifugation represents only one type of particle packing. It is not certain as to whether either one determines the true value of maximum packing fraction (Dabak and Yucel, 1986). However, it appears to be correct if the maximum packing fraction coming from sedimentation is employed for normalizing Newtonian suspension data such as high-shear and low-shear data without any yield stress being involved. For yield stress estimation, maximum packing fraction should be a variable that varies with the type of particle packing, and in turn with the state of suspension aggregation.

Model fitting

A number of rheological models has been proposed in an attempt to correlate relative viscosity of a concentrated suspension with its volume concentration (Eiler, 1941; Mooney, 1951; Maron and Pierce, 1956; Krieger and Dougherty, 1959; Frankel and Acrivas, 1967; Chong et al., 1971; Quemada, 1977; Wildemuth and Williams, 1984; Dabak and Yucel, 1986). In order to accommodate data beyond the dilute limit, maximum packing fraction is usually incorporated into these models. Fitting measured data into a suitable model for nonlinear curve fitting to obtain the maximum packing fraction of a concentrated suspension is a convenient method and is frequently used. The accuracy of the maximum packing fraction obtained obviously depends on the reliability of experimental data and the suitability of the rheological model chosen, because all models are only successful over a certain concentration region and for some particular suspensions. Relevant features of the model, such as shear level, range of volume concentration and number of model parameters, should therefore be taken into account in finding an appropriate model for the situation under investigation.

It is worth noting that the maximum packing fraction obtained by this method corresponds only to a certain shear level and hence to a certain state of suspension aggregation, because data of $(\eta_r - \phi)$ is fitted at a fixed shear rate or shear stress. Maximum packing fraction as a function of shear can be found by fixing different values of shear rate or shear stress on several flow curves containing various volume concentrations.

Effect of main factors on maximum packing fraction

Shape and size of suspended particles

The maximum packing fraction of a concentrated suspension is very sensitive to the characteristics of suspended particles and is controlled by the type of particle packing. Particle asymmetry is one key factor. Different packing efficiencies due to various shapes of particles lead thus to quite different values of maximum packing fraction.

The maximum packing fraction is found to be independent of particle size for a mono-dispersed system (Chong et al., 1971; Krieger, 1972) and it is not sensitive to particle size in a system of narrow size distribution (Metzner, 1985). A substantial effect of particle size on maximum packing fraction could, however, occur in an aggregated system containing very fine particles in which Brownian motion (diffusion effect) or particle-particle interactions become dominant, in particular, at low shear level.

Size distribution of suspended particles

The most significant factor affecting the maximum packing fraction of highly concentrated suspensions is distribution of particle size. The value of the maximum packing fraction increases gradually from mono-dispersed particle systems to multi-dispersed particle systems because smaller particles can fit into the voids between the bigger ones. An extremely high maximum packing fraction can be achieved by using an infinitely polydispersed particle system at high shear levels. However, in practice, the range of particle size is finite. Therefore, Metzner (1985) suggested that a trimodal particle size distribution may be the best one could normally employ, and Probstein et al. (1994) successfully described the rheological behaviour of a polydispersed suspension with a particle size distribution from submicrometer to hundreds of micrometers only by employing a bimodal model and a maximum packing fraction that is obtained directly from viscosity measurements of bidispersed suspensions.

Particle-particle interactions

The effect of particle-particle interactions on the value of maximum packing fraction is due to the variable amount of suspending medium trapped by aggregates and various packing-arrangements of aggregates formed by interparticle interactions. The value of the maximum packing fraction is therefore closely related to the state of suspension aggregation as a result of interactions between suspended particles. Flocculated suspension has a lower efficiency in particle packing, hence lower ϕ_m. Dispersed suspension has a higher packing efficiency, thus higher ϕ_m. Aggregated suspension can have similar rheological properties to flocculated suspension without sacrificing efficiency in particle packing. In addition, the features of the suspending medium also play a crucial role in providing an environment where particle-particle interactions may be promoted or inhibited besides the substan-

tial effects of suspended particle characteristics on the nature and degree of the suspension aggregation.

Hydrodynamic effect

The maximum packing fraction determined by the aggregate state of a concentrated suspension depends very much upon external shear because hydrodynamic forces induced by shear can break up the structure of aggregates or change the arrangement of aggregates. At low shear, interparticle forces are dominant, aggregates trap more medium and the state of aggregation is looser, hence lowering ϕ_m. At higher shear, hydrodynamic forces become dominant, more medium is released from aggregates and the state of aggregation is denser, thus resulting in a higher ϕ_m. At extremely high shear, all aggregates are destroyed except for those permanent agglomerates constructed of oppositely charged particles. Under these conditions all particulates tend to be more ordered, hence the closest packing having much higher ϕ_m is formed. An aggregated suspension undergoes disaggregation and ordering with increase of shear intensity, so ϕ_m increases with increasing shear.

Clearly ϕ_m, as a shear-dependent variable that is substantially affected by interparticulate interactions, is a powerful indicator of the resulting state of aggregation, and plays the dominant role in determining the behaviour of a highly concentrated suspension. By using ϕ_m, the arrangement of aggregates and the packing type for particles in the suspension may be related to almost all properties of concentrated suspension constituents in terms of the influences discussed above. It should also be noted that ϕ_m may be correlated with either shear rate, or shear stress, so it is necessary to test which of these is the more relevant variable for investigation.

Estimation of yield stress from shear-dependent ϕ_m

Principal equations for yield stress estimation

Maximum packing fraction determination

In order to obtain the shear-dependent ϕ_m of a concentrated suspension, the following equation originally proposed by Krieger and Dougherty (1959) for rigid sphere suspensions is employed:

$$\eta_r = \frac{\eta}{\eta_s} = \left(1 - \frac{\phi}{\phi_m}\right)^{-[\eta]\phi_m} \tag{1}$$

Here both maximum packing fraction ϕ_m and intrinsic viscosity $[\eta]$ are considered to be dependent on shear stress. Putting $n = [\eta]\phi_m$ in Eq. (1) results in an alternative due to Dabak and Yucel (1986):

$$\eta_r = \frac{\eta}{\eta_s} = \left(1 + \frac{[\eta]}{n}\,\frac{\phi}{1-\phi/\phi_m}\right)^{n} \tag{2}$$

Here exponent n reflects the level of interparticle forces acting between particles and varies with shear stress as well.

Using either of the equations above, the value of maximum packing fraction as a function of shear stress can be readily obtained by trial and error and by means of least-squares fitting of relative viscosity data as a function of volume concentration. The shear-dependent intrinsic viscosities and exponents can also be found at the same time.

Structural parameter λ

In order to relate shear-dependent ϕ_m to the actual state of suspension aggregation, the following equation is used first introduced by Quemada (1984).

$$\frac{1}{\phi_m} = \frac{1}{\phi_{m.\infty}} + \left(\frac{1}{\phi_{m.0}} - \frac{1}{\phi_{m.\infty}}\right)\lambda \tag{3}$$

where λ is a structural parameter that represents the dynamic equilibrium of whole suspension architecture under the balance of relevant forces. $\phi_{m.0}$ and $\phi_{m.\infty}$ are limiting maximum packing fractions that respectively correspond to solid-like state ($\lambda = 1$) and liquid-like state ($\lambda = 0$). As a result, the actual state of suspension aggregation is quantitatively represented by λ.

Reversible kinetic equation

In order to present the relationship between the state of aggregation of a concentrated suspension and the balance of forces involved, a rate equation is used in which different kinetic orders can be introduced for aggregation and disaggregation, and by which the competition of relevant forces can be demonstrated:

$$\frac{d\lambda}{dt} = \frac{(1-\lambda)^{\alpha}}{k_A} - \frac{\lambda^{\beta}}{k_S} \tag{4}$$

Here $1/k_A$ and $1/k_S$ are the rate coefficients for aggregation and break-down of suspension structure, respectively, and may be closely associated with the features of forces involved in architectural change of the concentrated suspension. Different relationships between λ and relevant forces can result from various kinetic orders (α, β). However, it is noted that change of orders does not significant-

Rheologica Acta, Vol. 34, No. 6 (1995)

ly affect the resultant relation in the equilibrium state. Consequently, once first order ($\alpha = \beta = 1$) is assumed for the aggregation-break down kinetics, the dynamic equilibrium state of suspension architecture becomes

$$\lambda = \frac{1}{1+\dfrac{1/k_S}{1/k_A}} \tag{5}$$

The state of a concentrated suspension depends on the balance between hydrodynamic forces that contribute to the break-down of the suspension structure and interparticulate forces that lead to aggregation of the suspension structure in the absence of Brownian motion. As a consequence, it is appropriate to assume the following dependence of rate constants on shear stress:

$$\frac{1/k_S}{1/k_A} = \left(\frac{\tau}{\tau_c}\right)^p \tag{6}$$

Here τ_c is a characteristic stress that reflects the strength of total interparticle interactions, and p is a model fitting parameter that reflects the sensitivity of the resulting state to the force balance.

Yield stress estimation

In order to correlate bulk properties of a concentrated suspension with the resulting architecture determined by the balance of hydrodynamic forces and interparticle forces, the following equation is derived by combining Eqs. (3), (5) and (6):

$$\frac{\dfrac{1}{\phi_m}-\dfrac{1}{\phi_{m.\infty}}}{\dfrac{1}{\phi_{m.0}}-\dfrac{1}{\phi_{m.\infty}}} = \frac{1}{1+\left(\dfrac{\tau}{\tau_c}\right)^p} \tag{7}$$

When the actual volume fraction ϕ of a concentrated suspension is between $\phi_{m.0}$ and $\phi_{m.\infty}$, decreasing shear stress on the suspension means ϕ_m decreases until it reaches ϕ, and η_r becomes infinite. At this point, the shear stress must be the yield stress τ_y of the suspension. Therefore, yield stress of a concentrated suspension can be determined by changing Eq. (7) into the following form:

$$\tau_y = \left[\left(\frac{\phi}{\phi_{m.0}}-1\right)\Big/\left(1-\frac{\phi}{\phi_{m.\infty}}\right)\right]^{1/p}\tau_c \ . \tag{8}$$

Physical meanings of the parameters

Parameter $\phi_{m.0}$, $\phi_{m.\infty}$

$\phi_{m.0}$ and $\phi_{m.\infty}$ are regarded as critical values because a concentrated suspension has a yield stress if its actual volume concentration falls into the range of $\phi_{m.0}$ to $\phi_{m.\infty}$. The value of $\phi_{m.0}$ may be viewed as a threshold from which the architecture of a concentrated suspension can sustain some external forces, and macroscopically, a certain stress has to be imposed on the suspension to initiate its movement. $\phi_{m.\infty}$ is a maximum volume concentration at which the yield stress of a concentrated suspension approaches infinity, and thus the suspension can no longer be moved at any applied stress.

$\phi_{m.0}$ and $\phi_{m.\infty}$ are considered to be limiting values corresponding to the actual architecture of a concentrated suspension and the structure of aggregates. $\phi_{m.0}$ is related to the low-shear state in which non-hydrodynamic forces are dominant, the architecture of the concentrated suspension is random and the structure of aggregates is looser. $\phi_{m.\infty}$ is related to the high-shear state in which hydrodynamic forces are dominant, the architecture of the concentrated suspension becomes much more ordered and the structure of aggregates becomes much denser, so that the concentrated suspension can not be moved any longer.

Clearly, $\phi_{m.0}$ and $\phi_{m.\infty}$ have explicit significance due to their having macroscopic manifestations as well as a microscopic explanation.

Parameter τ_c

τ_c may be considered as a quantitative representation of total interparticulate cohesion that competes against hydrodynamic forces (F_H) in determining the architecture of suspensions and structure of aggregates. The dimensionless ratio τ/τ_c reflects the relative importance of imposed shear stress and total cohesion existing between particles. The interparticulate force (F_C) acting on a pair of particles may contain two major contributions; i.e., particle interactions stemming from van der Waals forces (F_A) and interactions resulting from electric double layer overlap (F_R). For like- or unlike-charge particle suspensions, τ/τ_c thus may plausibly be assumed to obey an equation such as:

$$\frac{\tau}{\tau_c} = C\cdot\frac{F_H}{F_C} = C\cdot\frac{F_H}{F_A \pm F_R} = C\cdot\frac{1}{F_A/F_H(1\pm F_R/F_A)} \tag{9}$$

$$\frac{F_A}{F_H} = N_{V.H} = \frac{A}{6\pi\mu\dot{\gamma}a^3} \tag{10}$$

$$\frac{F_R}{F_A} = N_{R.V} = \frac{\varepsilon_r \varepsilon_0 \psi_0^2 a}{A} \quad (11)$$

The dimensionless ratios $N_{V.H}$ and $N_{R.V}$ are defined as the ratio of the magnitude of van der Waals forces to the magnitude of the hydrodynamic forces and the ratio of the electrostatic particle interaction forces to van der Waals forces respectively (Greene et al., 1994). A is the Hamaker constant; parameter a is taken as the averge particle radius based on a specific surface that is extremely important for particle-particle interactions; ε_r is the relative dielectric constant of medium; ε_0 is the dielectric constant of vacuum; ψ_0 is a constant surface potential of particles; μ is the viscosity of the medium and $\dot{\gamma}$ is shear rate. C is a factor that reflects the difference between two-particle interaction and multi-particle interactions. The $\pm$ sign occurs because F_R could be attractive or repulsive interactions depending on the circumstances under consideration.

A method is adopted similar to that used by Krieger and Dougherty (1959) who proposed that particles in solid-liquid suspensions virtually interacted via the suspension as a whole rather than through the liquid medium. Viscosity of the suspensions (η), therefore, should replace viscosity of medium (μ) in Eq. (10). In addition, to a first approximation, ψ_0 may be taken to be equal to the zeta-potential (ζ) of particles. Consequently, τ_c can be obtained:

$$\tau_c = \frac{1}{6C\pi a^3} \cdot (A \pm \varepsilon_r \varepsilon_0 \zeta^2 a) \quad (12)$$

Parameter p

The exponent p may be regarded as an indicator that reflects the response of the aggregate state to shearing, and may be closely related to the sensitivity of the suspension equilibrium state to the balance of shear stress and total interparticulate interaction forces.

Experimental

Materials and preparation of suspensions

Nine series of solid-liquid suspensions and one series of cocoa in fat suspension, as shown in Table 1, were utilised for this study. The composition of the solid-liquid suspensions is primarily silica flour with metal oxides such as titanium, ferric and aluminium. All materials are commercially available. Owing to charge difference, oxides may be adsorbed on to silica surfaces by which particle aggregation can be promoted so that serious settling may be reduced substantially. A very small quantity of aluminium sulphate $Al_2(SO_4)_3$ (analytical reagent grade) was mixed with SWA suspension to prevent silica particles from settling too rapidly. A minute quantity of sodium tripolyphosphate $Na_5P_3O_{10}$ (technical grade) was added into STW5 suspension as a dispersing agent for comparison. A small amount of potassium chloride KCl (analytical reagent grade) was put into STW4 suspension

Table 1 Details of experimental suspensions

Suspension series	Composition		Suspending medium viscosity (Pa·s)	Supernatant pH value	Supernatant ionic strength	Chemical additive
	Suspended solid	Suspending medium				
SGW	SiO_2*	84.2% (wt) aqueous solution of glycerine	0.077	3.6		
SWA	SiO_2*	Distilled water	0.001	4.8 ± 0.2		0.09% (wt) aluminum sulphate
STW1	TiO_2/SiO_2* = 0.14 wt	Distilled water	0.001	6.3		
STW2	TiO_2/SiO_2* = 0.08 wt	Distilled water	0.001	6.2		
STW3	TiO_2/SiO_2† = 0.14 wt	Distilled water	0.001	5.75 ± 0.15		
STW4	TiO_2/SiO_2† = 0.08 wt	Distilled water	0.001	5.3	0.2 moles/litre KCl	26.9 g potassium chloride
STW5	TiO_2/SiO_2† = 0.14 wt	Distilled water	0.001	5.8 ± 0.2		42 ppm sodium-tripolyphosphate
SAW	Al_2O_3/SiO_2† = 20 wt	Distilled water	0.001	6.2 ± 0.2		
SFW	Fe_2O_3/SiO_2† = 9.0 wt	Distilled water	0.001	7.3 ± 0.2		
COF	Cocoa powder	Cocoa fat	0.0217	not applicable	not applicable	

* QFF silica flour
† 400WQ silica flour

Rheologica Acta, Vol. 34, No. 6 (1995)

Table 2 Analysis of solid particle size

Materials	Supplied by	Grade	Analysis conditions	Average diameter (volume) (μm)	Average diameter (specific surface) (μm)	Size distribution (μm)			Span $\frac{D_{>90}-D_{<10}}{D_{50}}$
						$D_{>90}$,	D_{50},	$D_{<10}$	
Silica flour	Commercial Minerals Ltd.	QFF	5 min ultrasonic	5.38	1.20	12.98	2.31	0.51	5.40
		400WQ	5 min ultrasonic	2.39	0.58	4.56	0.96	0.24	4.52
Titanium dioxide	Tioxide Australia Pty. Ltd.	R-HD2	5 min ultrasonic	0.97	0.47	1.96	0.66	0.22	2.64
Ferric sesquioxide	Brazil		40 min stirring	5.98	1.51	15.64	3.04	0.68	4.93
Alumina trihydrate	Commercial Minerals Ltd.	AH20	5 min ultrasonic	11.55	3.70	25.63	7.89	1.74	3.03
			0.1 mg/litre, Na_4-pyrophosphate 5 min ultrasonic	11.52	3.71	24.79	8.38	1.71	2.75
Cocoa powder	Da-Ming Oil and Food Co.					18.7	13.1	6.09	0.963

to investigate ionic strength effects in the suspending medium.

Viscosity of glycerine solution as a suspending medium in SGW suspension was determined by means of contraves rheometers (Low-shear 30 and Rheomat 30). The pH value of each suspension supernatant was measured after the pH of the suspension was adjusted by adding either 1 M NaOH solution or 1 M HCl solution.

The size distributions of particles constituting the test suspensions, except cocoa powder, were analysed by means of a Malvern Mastersizer/E. The size distribution of cocoa powder was determined with a Brookhaven BI-90 particle sizer. The results obtained and the conditions applied are given in Table 2.

All stock suspensions were prepared in a similar way. The suspended particles, except cocoa powder which is dried at 80 °C for about 2 h, were first dried at ~110 °C for approximately 12 h. The particles were then mixed with an approximately equal mass of distilled water in a 5-litre bucket after the dry particles were cooled down to room temperature. The mixture was intensively stirred for 1 h to break up loosely agglomerated particles, then gently stirred for 5 days to ensure uniform suspension before any measurements or property modifications were carried out.

Test samples were taken from the stock suspension, and different volume fractions of solid ϕ were obtained by sedimentation. A centrifuge was used to obtain the most concentrated samples. Each sample was thoroughly stirred before being transferred to the rheometer or used for concentration measurement. The volume fraction ϕ was determined by a standard filtration/drying method (ASTM 1975).

Instruments and methods

The rheometers used in this work were Haake models RV3, RV12, RV20 and a contraves Rheomat 30. Brabender rheometer made by ECUST was employed for cocoa-fat suspension after being calibrated with silicone oils. Profiled concentric-cylinder system was chosen as a measuring system to avoid wall slip and provide minimal error when slight settling of test suspension occurs (Collins and Hoffmann, 1979).

A water jacket surrounding the measuring system was used to keep the test sample at a constant temperature, i.e., 60 °C for cocoa-fat suspension and 20 °C for the rest. A chart recorder was utilized to plot the response of torque reading at each rotational speed to ensure that the equilibrium state was obtained. The procedure of Krieger and Maron (1954) was used to evaluate the shear rate from rotational speed.

Results and discussion

Shearing effect

Relevant variables

The data of relative viscosity versus shear rate or shear stress, for the SGW series, was used to obtain extrapolated ϕ_m to examine whether shear rate was the relevant variable or shear stress. It was found (Fig. 1) that the values of ϕ_m can not be simply correlated with shear rate, and indeed it was almost independent of shear rate or decreased slightly with increasing shear rate. On the other hand, ϕ_m is reasonably correlated with shear stress.

The possible reason for this phenomenon, which also was found by Wildemuth and Williams (1985), is that the effect of suspension viscosity on hydrodynamic forces in a solid-liquid system is much greater than that of viscosity of the liquid alone. The latter is critical in other systems such as polymer solutions and emulsions. Consequently, shear stress ($\eta \cdot \dot{\gamma}$) becomes the relevant variable under the current conditions.

In view of this, relative viscosity was correlated in terms of shear stress. The curves of η_r versus τ for all series of suspensions under equilibrium conditions are shown in Figs. 2–10. The four curves containing lower volume concentrations in Fig. 9 were obtained by repeatedly immersing a rotating cylinder into the test suspensions that were loaded in a 1-litre beaker and had just finished stirring. In this way, the effect of serious settling on the measurements at such low volume concentration may be reduced. The analysis for a rotating cylinder in an infinite fluid was then used to obtain the viscosity.

Shear-dependent ϕ_m

The value of ϕ_m at a fixed shear stress for each suspension series was determined by means of the model fitting method. Several published models were used to fit the data of η_r and corresponding ϕ under fixed τ. It is of interest to note that the value of ϕ_m was not very sensitive to the model chosen. Probstein et al. (1994) also found that the choice of the viscosity expression was not critical in the determination of ϕ_m. Therefore, Eq. (1) derived by Krieger and Dougherty (1959) was fitted to the $\eta_r - \tau$ family of curves at constant shear stress for all series of suspensions because Eq. (1) gave the highest correlation coefficient among the models tried.

The fit for all series of suspensions, as shown in Figs. 11 and 12, is reasonably good except for the combination of high shear and low ϕ. Negative scatter was observed (e.g., SGW series) probably due to slight settling of the samples at very low concentration. As a result, the relative viscosity became lower with time. This would have produced a maximum effect in the high-shear results which were taken last. Positive scatter was also found (e.g., STW1 series) perhaps owing to the onset of secondary flows for samples having low concentration under very high speeds. Consequently, the relative viscosity was higher than it should have been. It is worth noting that the attainment of a state of true equilibrium of a concentrated suspension having high cohesive strength is tedious

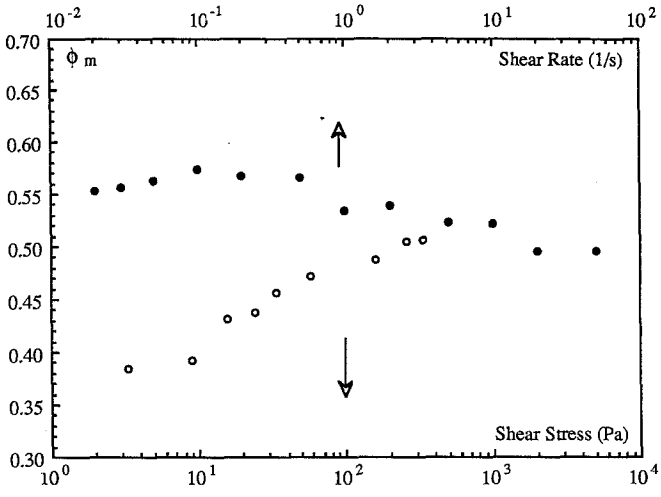

Fig. 1 Values of maximum packing fraction as a function of shear rate (upper results) and shear stress (lower results) for SGW series

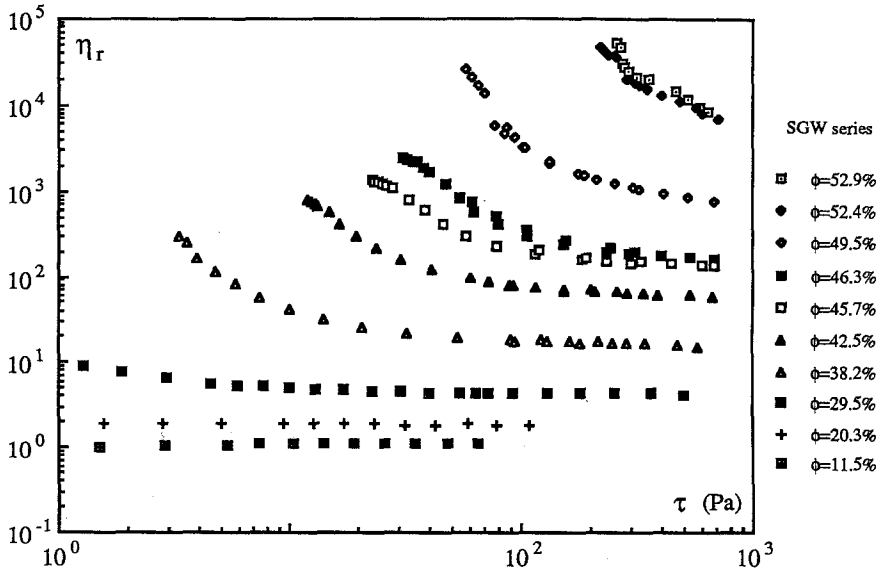

Fig. 2 Relative viscosity changes with shear stress at various volume concentrations

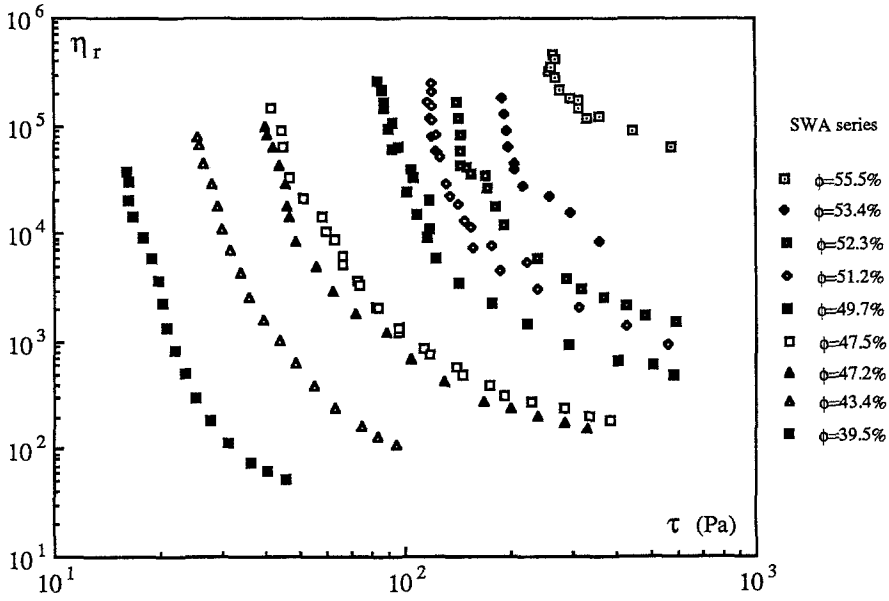

Fig. 3 Relative viscosity changes with shear stress at various volume concentrations

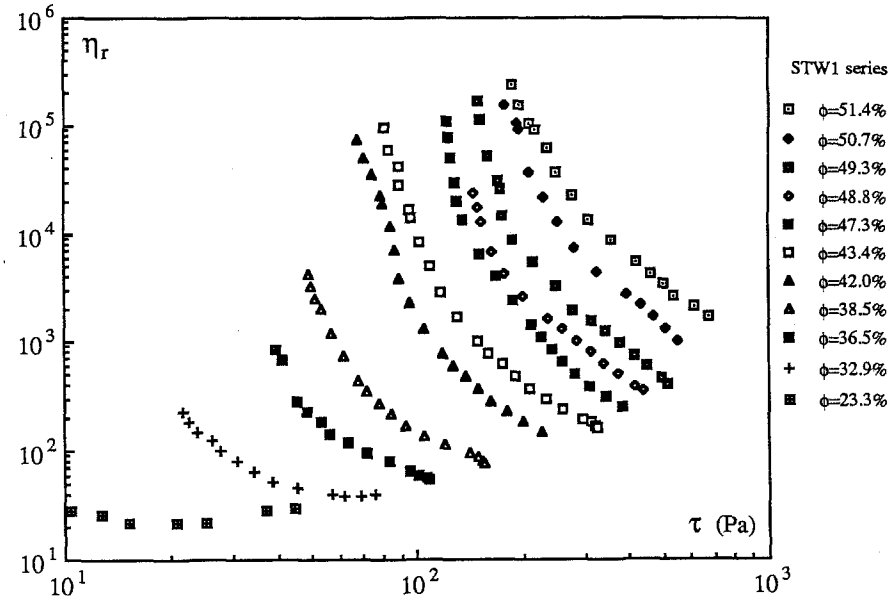

Fig. 4 Relative viscosity changes with shear stress at various volume concentrations

and time-consuming. Care should be taken to ensure the equilibrium state is reached. As can be seen from Figs. 11 and 12, excellent agreement between the model and experimental data of the samples at high concentration under lower shear is obtained. The use of a chart-recorder enabled the equilibrium state to be simply confirmed.

The values of ϕ_m obtained from model fitting at constant shear stress are plotted against that shear stress in Figs. 13 and 14 for all series of suspensions. The smooth curves on the figures represent Eq. (7) with $\phi_{m,0}$, $\phi_{m,\infty}$, p, τ_c parameters obtained by non-linear curve fitting to obtain the highest correlation coefficient. Table 3 lists the ranges of variables covered in the experiments and the parameters fitted to the results.

As expected, Fig. 15 shows that the curves of all series of suspensions collapse together if the structure parameter λ is plotted against the dimensionless variable $(\tau/\tau_c)^p$. This strongly indicates that the assumed reversible kinetics is adequate for describing the suspensions used in this investigation.

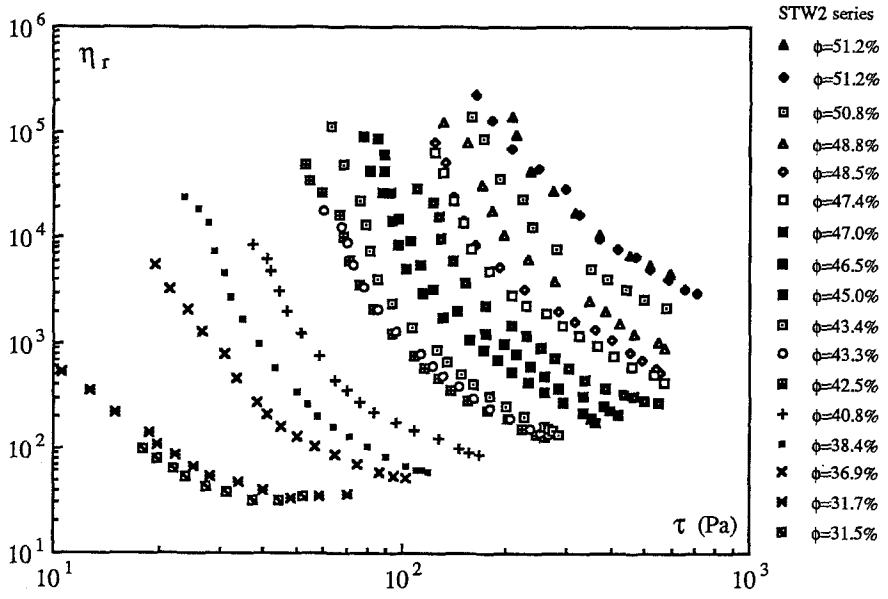

Fig. 5 Relative viscosity changes with shear stress at various volume concentrations

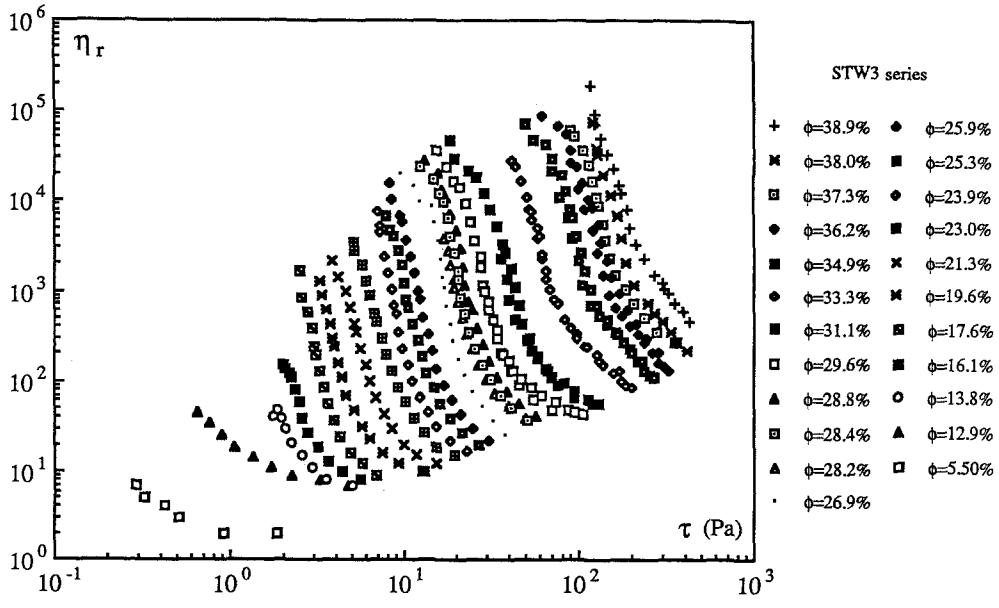

Fig. 6 Relative viscosity changes with shear stress at various volume concentrations

Characteristics of suspended particles

Shape of particles

The "particles" (i.e., aggregates) being studied are kinetic units that were obtained reproducibly by relatively mild agitation and were not easily destroyed by severe agitation. The shapes of these particles, except for cocoa powder which consisted of non-spherical particles, were thus taken to be either spherical or analogous to spheres having aspect ratio (L/D) close to one. Titanium dioxide, for example, is highly agglomerated in the dry state. The primary size of particles of TiO_2 lies in the range 0.05 to 0.40 μm (data provided by supplier). Obviously, as shown in Table 2, these sizes are much smaller than the size measured by a Malvern Mastersizer/E. The shape of the kinetic unit agglomerated from primary particles is more likely to approach spherical shape. Therefore, the agglomerate unit is assumed to be a spherical particle in this study.

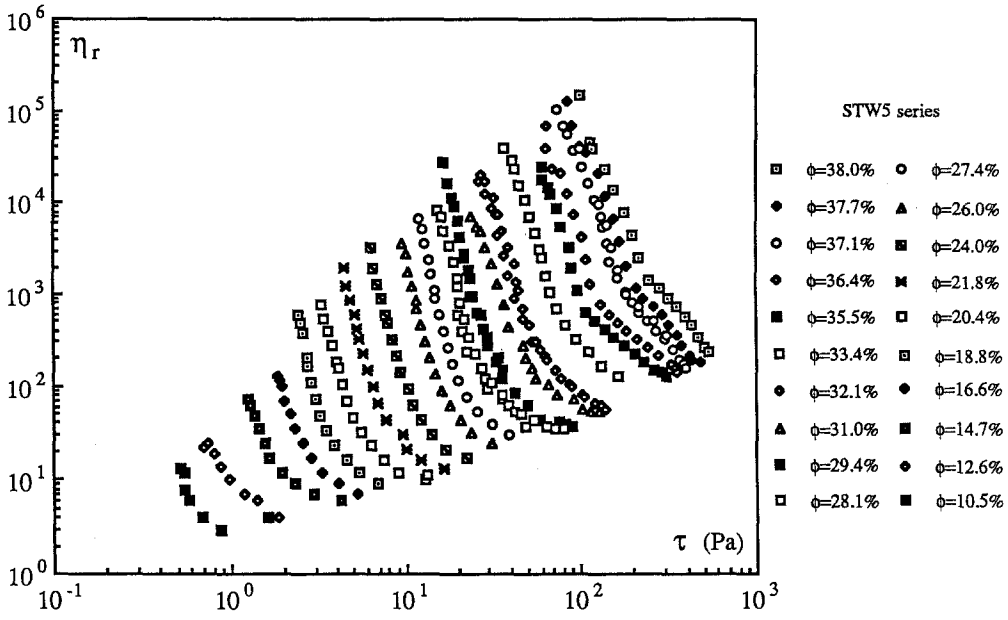

Fig. 7 Relative viscosity changes with shear stress at various volume concentrations

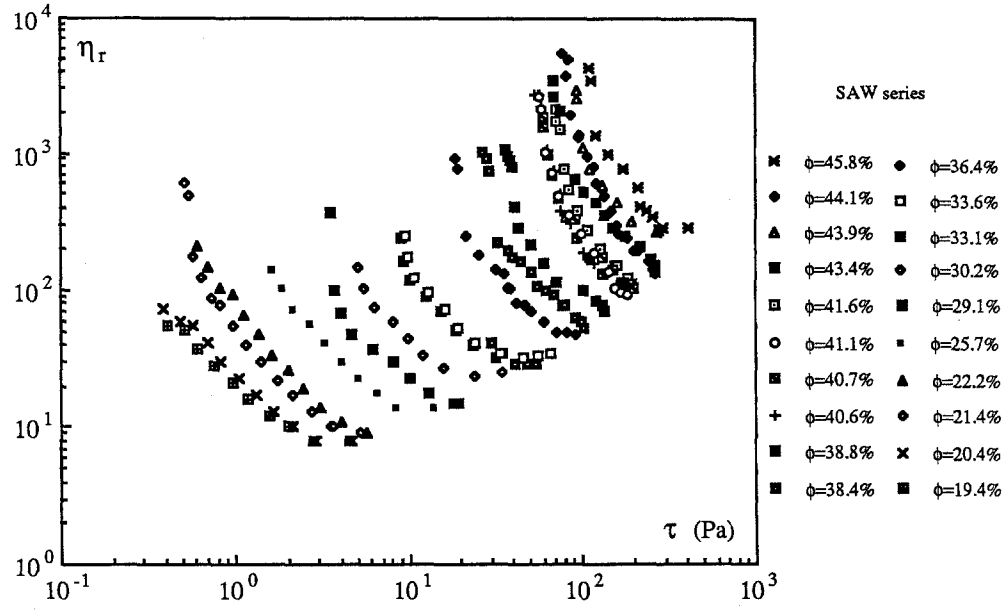

Fig. 8 Relative viscosity changes with shear stress at various volume concentrations

Distribution of particle size

The distributions of particle size are not very broad, but correspond to polydispersity according to the span defined as $(D_{>90}-D_{<10})/D_{50}$. Both STW1 series and STW 3 series contained oppositely-charged particles and were expected to be in mutual aggregation. The span of entity size distribution was found to be 6.67 for STW1 series and 4.88 for STW3 series respectively. As expected, the value of $\phi_{m,\infty}$ from STW1 series is larger than that from STW3 series. Clearly, $\phi_{m,\infty}$ depends mainly upon the size distribution of entities that persist after very high shear where hydrodynamic forces are dominant. The broader the distribution of entity size, the larger the value of $\phi_{m,\infty}$. However, an "anomalous" result can be observed if the values of $\phi_{m,\infty}$ from STW1 series and SWA series are compared to each other. The span of entity size distribution was 5.4 for SWA series which contains only one kind of particle. Unexpectedly, the $\phi_{m,\infty}$ from STW1 series was smaller than that from SWA series. This anomaly, in fact, derives from the aggregate state being changed from double layer overlap to permanent agglom-

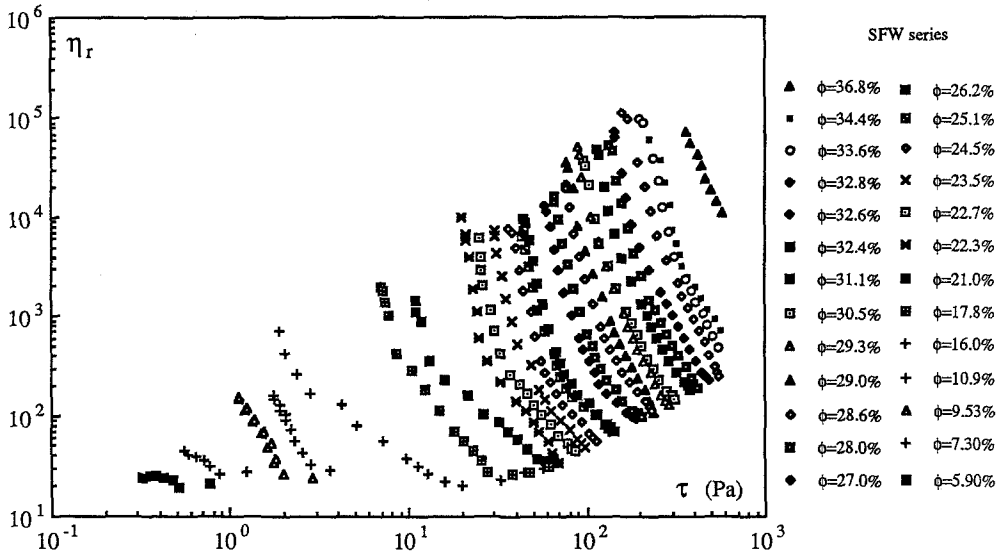

Fig. 9 Relative viscosity changes with shear stress at various volume concentrations

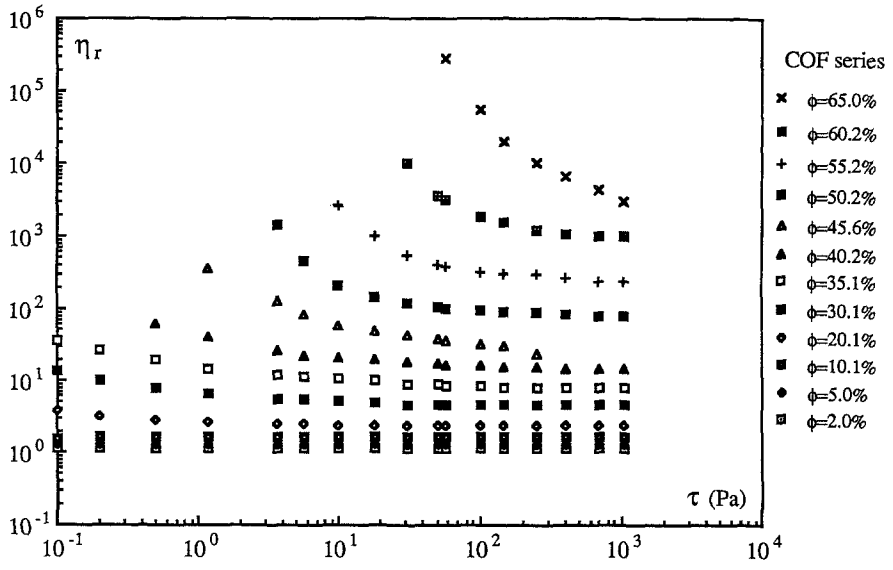

Fig. 10 Relative viscosity changes with shear stress at various volume concentrations

erate in which those aggregative groups attached by opposite electric-charge survived under high shear. The particles of TiO_2 in STW1 series, being mutually aggregated, have resulted in a significant effect on the state of aggregation. It is so significant that the increase in ϕ_m related to a broader entity size distribution is completely counteracted. In addition, it is observed that the quite large rheological difference between SWA series and STW1 series is due to the distribution of entity size rather than to entity size itself judging from the very small variation of mean entity size ($D_v = 5.38$ μm for SWA series and $D_v = 5.37$ μm for STW1 series respectively).

Features of suspending medium

Viscosity

The viscosity of the suspending medium influences the dispersion and permeation of particles. It is more difficult for aggregation and segregation to occur between particles in a higher viscosity medium. This is shown in Table 3 by the SGW series in glycerine in which ϕ_{m0} is larger and $\phi_{m\infty}$ is smaller than for the SWA series in water. The shear-effect on the architectural change of the suspension with a medium of higher viscosity is less pronounced due to the presence of stronger hydrodynamic forces and weaker strength of aggregation, so that in

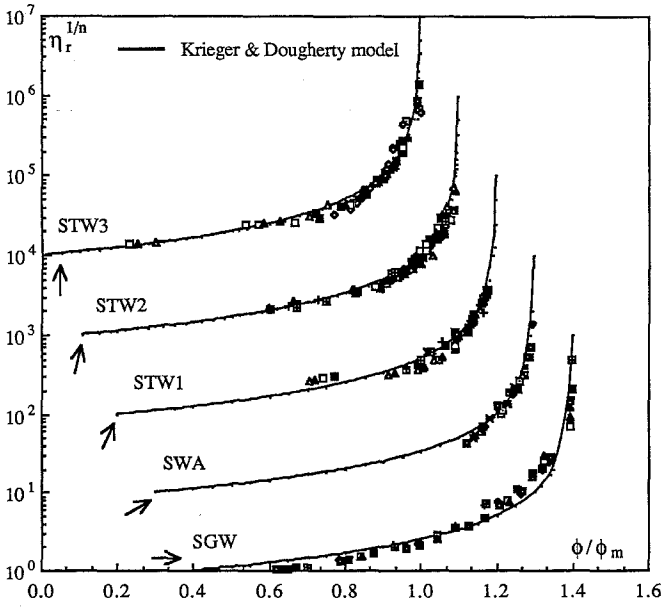

Fig. 11 Model fitting for data of relative viscosity vs. volume concentration (the origin of each curve has been moved to make a clear view)

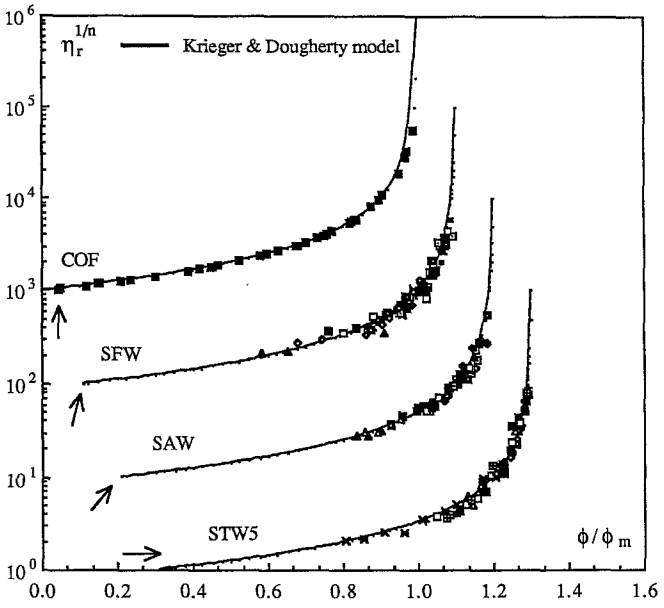

Fig. 12 Model fitting for data of relative viscosity vs. volume concentration (the origin of each curve has been moved to make a clear view)

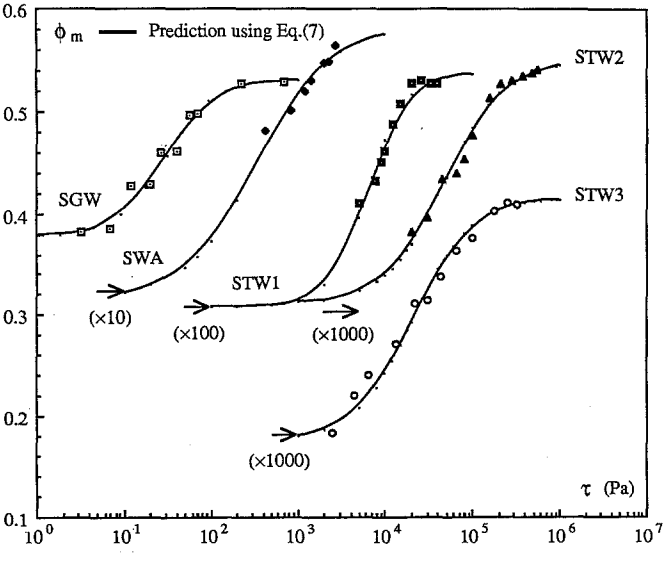

Fig. 13 Shear dependence of maximum packing fraction (the curves of SWA, STW1, STW2 and STW3 have been moved toward right to make a clear view)

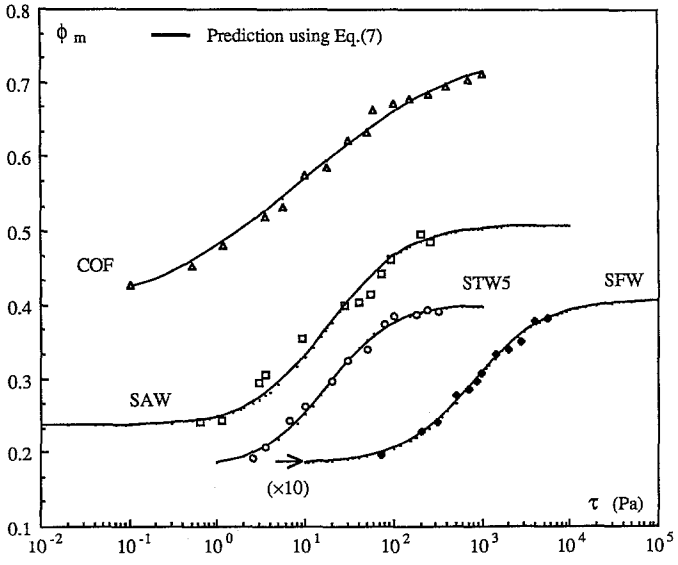

Fig. 14 Shear dependence of maximum packing fraction (the curve of SFW has been moved toward right to make a clear view)

SGW series, the range of ϕ_m is smaller than for the other series.

pH value

The isoelectric points (IEP) of the particles used in this study are shown in Table 4. The pH values of the suspensions containing dissimilar particles were intentionally adjusted to a intermediate value. As a consequence, the mutual aggregation between the particles took place due to interactions between the electric double layers of unlike-charge particles under the pH condition used. It is of interest to note that for suspensions having almost same pH values, such as STW1 series and STW2 series, the strength of aggregation depends only on the quanti-

Table 3 Summary of results from suspensions studied

Suspension type	Experiment range τ (Pa)	Krieger & Dougherty model				Quemada model	First-order kinetics
		Selection range τ (Pa)	Range of			$\phi_{m,0}$	p
			ϕ_m	$[\eta]$	$[\eta]\phi_m$	$\phi_{m,\infty}$	τ_c (Pa)
SGW	1.3 ~ 710	3.3 ~ 700	0.383	2.40	0.92	**0.378**	1.566
			0.529	4.00	2.10	**0.531**	**23.64**
SWA	2.4 ~ 587	42.0 ~ 268	0.481	5.04	2.52	**0.317**	1.072
			0.564	5.79	3.24	**0.582**	**19.23**
STW1	9.2 ~ 679	50.0 ~ 400	0.410	4.57	2.42	**0.308**	1.979
			0.531	6.87	3.29	**0.538**	**47.62**
STW2	1.6 ~ 707	20.0 ~ 550	0.383	5.33	2.52	**0.311**	1.300
			0.541	6.71	3.26	**0.550**	**30.30**
STW3	0.3 ~ 416	2.5 ~ 320	0.183	5.6	1.887	**0.177**	1.346
			0.410	10.4	2.73	**0.415**	**11.04**
STW4	9.7 ~ 306	Insufficient data to evaluate these parameters					
STW5	0.5 ~ 538	2.5 ~ 320	0.191	4.93	1.45	**0.181**	1.263
			0.393	7.63	2.70	**0.400**	**9.711**
SAW	0.4 ~ 412	0.62 ~ 260	0.242	4.48	1.77	**0.236**	1.024
			0.496	9.05	2.54	**0.508**	**8.873**
SFW	0.4 ~ 574	7.1 ~ 550	0.197	7.511	2.40	**0.184**	1.080
			0.382	16.06	3.17	**0.407**	**38.59**
COF	0.1 ~ 1028	0.2 ~ 700	0.43	4.2	1.9	**0.39**	0.482
			0.73	4.7	3.3	**0.75**	**2.61**

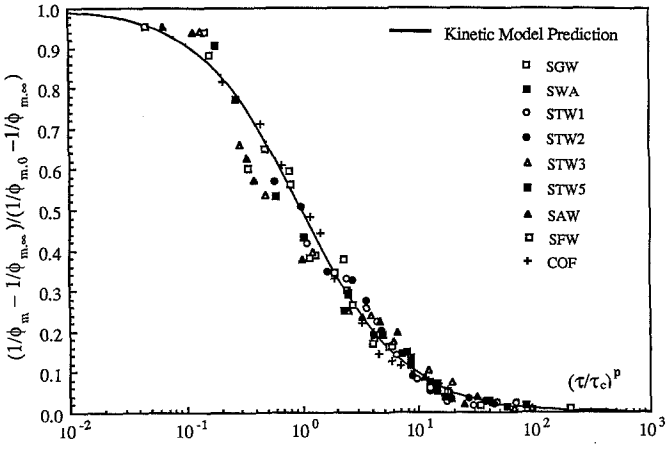

Fig. 15 Shear dependence of structural parameter λ

Table 4 Isoelectric points of particles and surface features

Particle type	pH value at isoelectric points†	pH = 6.3 T = 25 °C	
		μ[a] (μm/s)/(V/cm)	ζ[b] (mV)
Al_2O_3	8.0 ± 0.2		
Fe_2O_3	8.7 ± 0.1		
SiO_2	2.0 ± 0.2	−5.53	−70.78
TiO_2	6.4 ± 0.1	+1.60	+20.48

† Parks (1965)
[a] Measured by Zeta Meter equipped with GT-1 Teflon cell, ZETA-METER Inc.
[b] Calculated in terms of Smoluchowski's equation ($\zeta = 12.8\ \mu$)

ties of TiO_2. The greater the proportion of TiO_2, the higher the strength of aggregation, resulting in decreasing $\phi_{m,0}$ and increasing τ_c.

It is also noted that for suspensions containing the same quantities of TiO_2, such as STW1 and STW3 series, the farther from IEP the pH value, the less strength the suspension has. Hence a higher $\phi_{m.0}$ and lower τ_c are obtained. But the $\phi_{m,0}$ of STW3 is smaller than that of STW1. This is because STW3 contains different grade silica flour from STW1. As a consequence, the use of smaller silica flour in STW3 not only reduces the span of particle size distribution, thus lowering $\phi_{m,\infty}$ but also makes aggregation between the particles easier due to comparable thickness of electric double layers, hence lowering $\phi_{m,0}$ as well. The variation of $\phi_{m,0}$ to $\phi_{m,\infty}$ for STW3 series is, however, still larger than that for STW1 series. It seems as if the amount of aggregates in STW3 is larger than that in STW1, but the strength of aggregation in STW3 is less tenacious than in STW1. The reason for this may be related to the following mechanism of aggregation between TiO_2 and SiO_2. In STW1 series, the

Rheologica Acta, Vol. 34, No. 6 (1995)

surfaces of SiO_2 particles were almost completely coated by smaller TiO_2 particles by means of the overlap of electric double layers of opposite charge. Rough calculation showed that total particle numbers and surface area of TiO_2 particles were much larger than that of SiO_2 particles. Further, the analysis of particle size distribution confirmed that the result of STW1 suspension entities is similar to that of silica flour alone. In general, the aggregation in STW1 resulted from the interactions between SiO_2 particles totally coated by TiO_2 particles and additional TiO_2 particles. Consequently, the surface features of TiO_2 particles are dominant for determining the state of STW1 aggregation, and the strength of aggregation in STW1 is high due to smaller ζ-potential resulting from an experimental pH value closed to the IEP of TiO_2 particles in terms of Eq. (12). In STW3 series, on the contrary, the total particle numbers and surface area of SiO_2 particles were a little larger than that of TiO_2 particles. Therefore, the strength of aggregation in STW3 is weaker due to relatively high ζ-potential stemming from an experimental pH value far from the IEPs of SiO_2 and TiO_2 particles.

Ionic strength

The ionic strength of suspending medium is thought to have a significant effect on the interactions between the suspended particles, and hence on the rheological properties of concentrated suspension. The van der Waals attraction decreases with increasing ionic strength of suspending medium because the Hamaker constant decreases in terms of Lifshit, equation (Israelachvili, 1985) due to the increase of the medium dielectric constant and refractive index. Moreover, the attractive interactions stemming from the overlap of electric double layers of opposite-charged particles also decrease due to the shrinkage of the layers. In this work, the pH values of two series of suspensions containing the same ratio TiO_2/SiO_2, namely, STW2 and STW4, were first adjusted to almost same value, i.e., 6.2 for STW2 and 6.1 for STW4. The suspension STW4 series was then increased in ionic strength by addition of KCl. Consequently, the ionic strength (0.2 moles/litre) of the STW4 series is much higher than that of the STW2 series ($\sim 10^{-5}$ moles/litre).

Figure 16 shows the dramatic change of the suspension viscosity owing to the increase of ionic strength. The volume concentrations of the suspensions from the STW4 series are higher than those from the STW2 series when the curves of relative viscosity versus shear stress are compared with each other. This clearly indicates that the higher ionic strength favours aggregation of the suspensions containing opposite-charged particles. Further, this promotion is more significant at high concentration level judging from the difference of the volume concentration between the three pairs of curves shown in Fig. 16. There

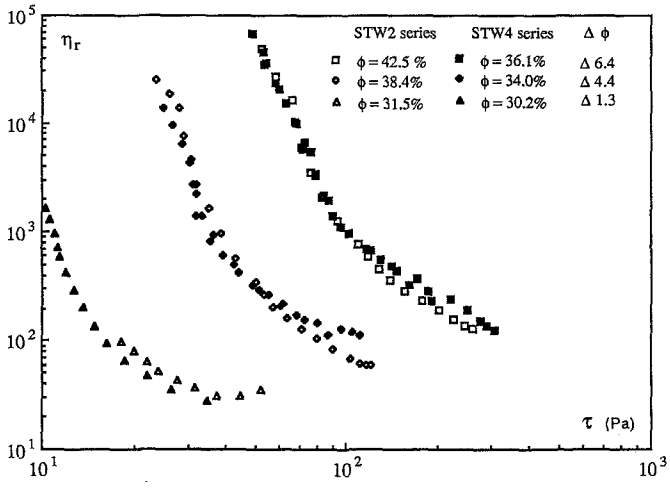

Fig. 16 Effect of ionic strength on the viscosity of suspensions containing opposite-charged particles

are two possible reasons for this. One is attraction stemming from van der Waals forces. The Hamaker constant decreases with increase of ionic strength of the medium, but the resulting van der Waals attraction depends both on the Hamaker constant and on the distance between the particle surfaces. Therefore, this attraction may increase at very high concentration when the ionic strength of the medium is increased. The other, more significant reason is the overlap of electric double layers. Although the effective extent of the layers is reduced because of their shrinkage resulting from higher ionic strength, the density of electric charge within the layers is increased. Strong attraction between particles easily occurs especially in highly concentrated suspensions owing to very small distance between the particles.

Interactions between solid particles

Relationship of τ_c and properties of suspension constituents

It seems reasonable that τ_c should be a quantitative measure of the strength of total interparticulate interactions. In view of what is shown earlier, τ_c is approximately directly proportional to Hamaker constant A, ζ-potential of particles at a given pH value, and inversely proportional to average size of particles. Unfortunately, τ_c value can not be estimated theoretically at this stage owing to the fact that no information could be obtained about the details of the aggregate arrangement in three dimensions in the suspensions (unknown parameter C in Eq. (12)). However, the Hamaker constant and the ratio of interactions due to double layer overlap to van der Waals attraction, can be evaluated in terms of Lifshitz equation

(Israelachvili, 1985) and Eq. (11). The Hamaker constant calculated from the Lifshitz equation is $3.17 \cdot 10^{-21}$ for SGW series, $1.39 \cdot 10^{-20}$ for SWA series and $5.78 \cdot 10^{-20}$ for STW1 series. The ratio of F_R to F_A evaluated from Eq. (12) is approximately -349 for SGW series, -362 for SWA series and $+17.1$ for STW1 series. Clearly, the particle interactions stemming from van der Waals forces are far less important than the interactions deriving from the overlap of electric double layers of like- or unlike-charge particles. Therefore, it can be concluded that the state of aggregation under the conditions here are dominated by the interactions introduced by the overlap of electric double layers at low shear level. These interactions are directly affected by dielectric constant of medium, average particle size and absolute value of ζ-potential of particles. Alternatively, the interactions are indirectly influenced by ionic strength and pH value of medium.

Dispersing agent

A very small amount of sodium tripolyphosphate, as a dispersing agent, was added into stock suspension to generate series STW5 in which the quantities of TiO_2 particles and pH value are almost the same as that of STW3 series. Sodium tripolyphosphate is known to be able to break up aggregates, release the trapped medium, and result in thinning owing to its high negative charge and high complexing affinity for free positive particles. Considerable suspension thinning occurred on addition of the dispersing agent. But after the initial thinning, the suspension viscosity increased again in time. As expected, the value of $\phi_{m,0}$ for STW5 is larger than that for STW3, and τ_c of STW5 is smaller than that of STW3. However, contrary to intuitive anticipation, $\phi_{m,\infty}$ of STW5 is smaller than that of STW3. This result suggests that the tiny amount of dispersing agent can only break up the general architecture of the suspension which is built by all pairs of TiO_2/SiO_2 aggregates but can not affect individual aggregates of TiO_2 and SiO_2 which result from the overlap of electric double layers of opposite charge. The suspension most likely restores its architecture when new surfaces of TiO_2 and SiO_2 aggregates become available to interact with one another. $\phi_{m,\infty}$ of STW5 thus is a little smaller than that of STW3 because high shear may provide more chances for replacing the surfaces of TiO_2 and SiO_2 aggregates and result in easier aggregate structuring, hence lowering $\phi_{m,\infty}$.

Comparison of model prediction and experimental evidence

The yield stress predicted by Eq. (8) is compared in Figs. 17 and 18 with the results of independent measurements, which were obtained by extrapolation to zero rotational speed of the flow curves (τ vs. rotational speed) or by vane torsion. The agreement is fairly good except for extremely high and relatively low concentrations. It is difficult to verify these predictions experimentally by means of only the measurements of flow curves and vane torsion, due to experimental limitations, such as settling at low concentrations, and unexpected rupture at extremely high concentrations. Rupture may be induced at points of structural weakness generated by entrapped air. This is in-

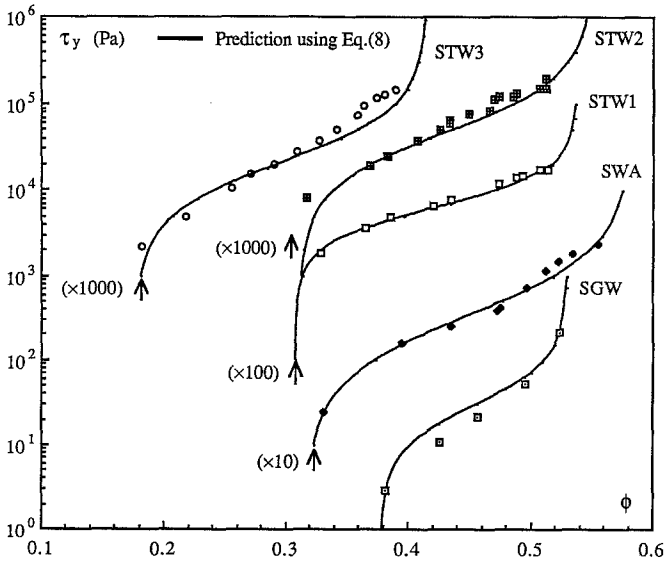

Fig. 17 Comparison of experimental observation and the model prediction for yield stress (the curves of SWA, STW1, STW2 and STW3 have been moved up to make a clear view)

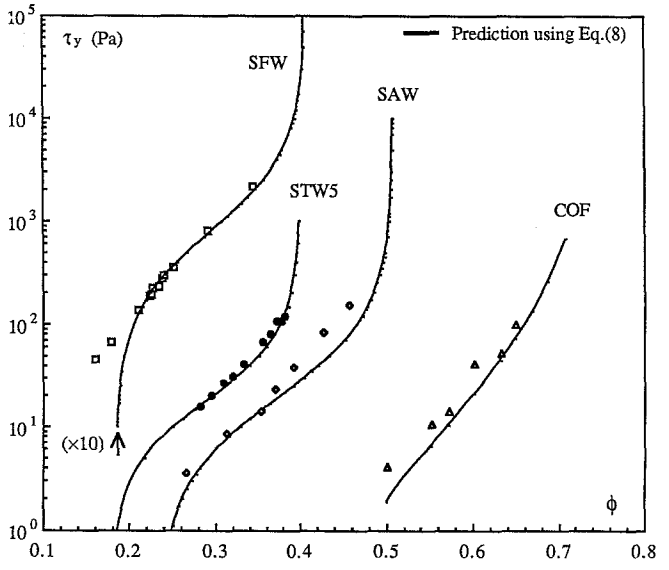

Fig. 18 Comparison of experimental observation and the model prediction for yield stress (the curve of SFW has been moved up to make a clear view)

creasingly difficult to avoid at extremely high concentrations.

Thomas (1961) first introduced a simple power-law equation for correlating yield stress with particulate volume fraction and selected the exponent to be 3. Wildemuth and Williams (1985) found that the proportionality of τ_y to ϕ^2 or ϕ^3 reported by Kao et al. (1975) and Castillo and Williams (1979) is not predicted in general, in particular because $\tau_y \to \infty$ at $\phi \to \phi_{m,\infty}$. A power-law form seems to correlate parts of the $\tau_y - \phi$ curve, but it is not able to satisfactorily describe the whole relationship between yield stress and ϕ in this work, as shown by the data for small volume concentrations in Fig. 16, for example. When a power law is fitted to the present data, the exponent varies from 4.9 to 12.9.

Conclusions

The rheological measurements for nine series of suspensions with remarkably different features have confirmed that the model proposed in this study is quite good for estimating the yield stress of concentrated suspensions of known volume fraction even though closer inspection is still needed to verify the model's validity at extremely high concentrations. Successful introduction of ϕ_m into the model has provided an opportunity to assess the effect of the properties of suspension constituents on the suspension architecture and aggregate structure.

It has been demonstrated that tailoring the rheological properties of concentrated suspensions is possible by changing and controlling the structure of the suspension using some operating variables, for example, pH value, ionic strength (salt concentration) and chemical additives such as dispersing or flocculating agents. Because aggregated suspensions have many advantages for improving actual processing in which serious settling needs to be eliminated and efficiency in particle packing needs to be maintained, the results presented here offer great potential for achieving this aim. The study has also shown that a scaling evaluation of interparticulate interactions can capture the most important effect which plays a decisive role in determining the behaviour of the suspensions, without knowning the details of three-dimensional arrangement of particles or aggregates.

Acknowledgements Financial support from the Australian Research Council, and from the China Natural Science Fund is gratefully acknowledged. Zhou also thanks Monash University for providing a Monash Graduate Scholarship.

References

Ackerson BJ (1990) Shear induced order and shear processing of model hard sphere suspensions. J Rheology 34: 553–590

ASTM (1975) Annual Book of ASTM Standards, part 19: "Natural building stones; soil and rock; peat, mosses, humus". Am Society for Testing and Materials

Buscall R (1991) Effect of long-range repulsive forces on the viscosity of concentrated latices: Comparison of experimental data with an effective hard-sphere model. J Chem Soc Faraday Trans 87:1365–1370

Castillo C, Williams MC (1979) Rheology of very concentrated coal suspensions. Chem Eng Commun 3:529–547

Chang CY, Powell RL (1994) Effect of particle size distributions on the rheology of concentrated bimodal suspensions. J Rheol 38:85–98

Chang SH, Ryan ME, Gupta RK (1993) The effect of pH, ionic strength, and temperature on the rheology and stability of aqueous clay suspensions. Rheol Acta 32:263–269

Chiu WY, Don TM (1989) A study on viscosity of suspensions. J Appl Poly Sci 37:2973–2986

Chong JS, Christiansen EB, Baer AD (1971) Rheology of concentrated suspensions. J Appl Poly Sci 15:2007–2021

Collins EA, Hoffmann DJ (1979) Rheology of PVC dispersions. J Colloid Interf Sci 71:21–29

Dabak T, Yucel O (1986) Shear viscosity behaviour of highly concentrated suspensions at low and high rates. Rheol Acta 25:527–533

Doraiswamy D, Mujumdar AN, Tsao I, Beris AN, Danforth SC, Metzner AB (1991) The Cox-Merz rule extended: A rheological model for concentrated suspensions and other materials with a yield stress. J Rheol 35:647–685

Eilers H (1941) Die Viskosität von Emulsionen hochviskoser Stoffe als Funktion der Konzentration. Kolloid Z Z Polym 97:313–321

Farris KJ (1968) Prediction of the viscosity of multimodal suspensions from unimodal viscosity data. Trans Soc Rheol 12:281–301

Frankel NA, Acrivos A (1967) On the viscosity of a concentrated suspension of solid spheres. Chem Eng Sci 22: 847–853

Frith WJ, Mewis J, Strivens TA (1987) Rheology of concentrated suspensions: Experimental investigations. Powder Technology 51:27–34

Greene MR, Hammer DA, Olbricht WL (1994) The effect of hydrodynamic flow field on colloidal stability. J Colloid Interf Sci 167:232–246

Israelachvili JN (1985) Intermolecular and surface forces. Academic Press

Kao SV, Nielsen LE, Hill CT (1975) Rheology of concentrated suspensions of spheres. I. Effect of the liquid-solid interface. J Colloid Interf Sci 53:358–373

Krieger IM, Dougherty TJ (1959) A mechanism for non-Newtonian flow in suspensions of rigid spheres. Trans Soc Rheol 3:137–152

Krieger IM, Maron SH (1954) Direct determination of the flow curves of non-Newtonian fluids. III. Standardized treatment of viscometric data. J Appl Phys 25:72–75

Krieger IM (1972) Advances in Colloid Interface Science 3:111–136

Lee DI (1970) Packing of spheres and its effect on the viscosity of suspensions. J Paint Technol 42:579–587

Leong YK, Boger DV (1990) Surface chemistry effects on concentrated suspension rheology. J Colloid Interf Sci 136: 249–256

Maron SH, Krieger IM (1960) Rheology Vol 3 (Ed. Eirich FR) Academic Press

Maron SH, Pierce PE (1956) Application of Ree-Eyring generalized flow theory to suspensions of spherical particles I. J Colloid Sci 11:80–95

Metzner AB (1985) Rheology of suspensions in polymeric liquids. J Rheol 29: 739–775

Mooney M (1951) The viscosity of a concentrated suspension of spherical particles. J Coll Sci 6:162–170

Nielsen LE (1977) Polymer Rheology, Chap 7. Marcel Dekker, New York

Parks GA (1965) The isoelectric points of solid oxides, solid hydroxides, and aqueous hydroxo complex systems. Chem Rev 65:177–198

Patton TC (1979) Paint flow and pigment dispersion. John Wiley & Sons Inc

Poslinski AJ, Ryan ME, Gupta RK, Seshadri SG, Frechette FJ (1988) Rheological behaviour of filled polymeric systems I. Yield stress and shear-thinning effects. J Rheol 32:703–735. Rheological behaviour of filled polymeric systems II. The effect of a bimodal size distribution of particulates. J Rheol 32:751–771

Probstein RF, Sengun MZ, Tseng T-C (1994) Bimodal model of concentrated suspension viscosity for distributed particle sizes. J Rheol 38:811–829

Quemada D (1984) Models for rheological behaviour of concentrated disperse media under shear. Proc IX Intl Congr Rheol, Mexico, 571–582

Quemada D (1977) Rheology of concentrated disperse systems and minimum energy dissipation principle I. Viscosity-concentration relationship. Rheol Acta 16:82–94

Russel WB (1980) Review of the role of colloidal forces in the rheology of suspensions. J Rheol 24:287–317

Sengun MZ, Probstein RF (1989) Bimodal model of slurry viscosity with application to coal-slurries. Part 1. Theory and experiment. Rheol Acta 28:382–393

Shapiro AP, Probstein RF (1992) Random packings of spheres and fluidity limits of monodisperse and bidisperse suspensions. Phys Rev Lett 68:1422–1425

Thomas DG (1961) III. Laminar-flow properties of flocculated suspensions. AIChE J 7:431–437

Tsai SC, Botts D, Plouff J (1992) Effects of particle properties on the rheology of concentrated noncolloidal suspensions. J Rheol 36:1291–1332

Tsai SC, Botts D, Viers B (1989) Effects of liquid viscosity on rheology of concentrated suspensions. Part Sci Tech 7: 87–95

Tsai SC, Viers B (1987) Effects of liquid polarity on rheology of noncolloidal suspensions. J Rheol 31:483–494

van der Werff JC, de Kruif CG (1989) Hard-sphere colloidal dispersions: The scaling of rheological properties with particle size, volume fraction and shear rate. J Rheol 33:421–454

Wildemuth CR, Williams MC (1984) Viscosity of suspensions modeled with a shear-dependent maximum packing fraction. Rheol Acta 23:627–635

Wildemuth CR, Williams MC (1985) A new interpretation of viscosity and yield stress in dense slurries: coal and other irregular particles. Rheol Acta 24:75–91